Article

The Impact of Lubricant Film Thickness and Ball Bearings Failures

Matthew Marko [1]*

Naval Air Warfare Center Aircraft Division   Joint-Base McGuire-Dix-Lakehurst, Lakehurst NJ 08733, USA
NAVAIR Public Release 2018-609 Distribution Statement A - "Approved for public release; distribution is
  unlimited"

*   Correspondence: matthew.marko@navy.mil

Abstract: An effort was made to find a relationship between the ratio of average asperities height and lubricant thickness at the point of contact of rolling element ball bearings, and empirical equations to predict the life for bearings under constant motion. Two independent failure mechanisms were considered, fatigue failure and lubricant failure resulting in seizing of the roller bearing. A theoretical formula for both of these methods was established for the combined probability of failure using both of these failure mechanisms. Fatigue failure was modeled with the empirical equations of Lundberg and Palmgren and standardized in DIN/ISO281. The seizure failure, which this effort sought to investigate, was predicted using Greenwood and Williamson's theories on surface roughness and asperities during lubricated contact. These two mechanisms were combined, and compared to predicted cycle lives of commercial roller bearing, and a clear correlation was demonstrated. This effort demonstrated that the Greenwood-Williams theories on the relative height of asperities versus lubricant film thickness can be used to predict the probability of a lubricant failure resulting in a roller bearing seizing during use.

Keywords: Lubrication, Ball Bearings, Roller Bearings, Failures, L10, Film Thickness

---

1. Introduction

Ball bearings are used in countless mechanical applications to convert sliding mechanical contact into rolling contact [1–3], dramatically reducing friction energy losses. Sliding contact inherently has a high friction force, as random asperities can contact the surface and induce wear and damage to machined parts [4–9]. Rolling contact, however, has dramatically lower friction; the overwhelming majority of the friction loss is merely hysteresis from elastic deflections of the circular bearings.

Rolling element bearings are one of the most common configuration of ball bearings, with the bearings contained in a circular race to allow continued circular motion. So long as there is a minimum surface friction to enable the bearings to roll, there will be a dramatic reduction in circular friction for an object spinning inside or outside of the races. Bearings can be spherical, cylindrical, or a host of different configurations depending on the applications of the ball bearings.

A well built bearing can last indefinitely, however all mechanical objects have some risk of failure. Despite the previous assumptions that stresses less than half of yield have no significant risk of failure, there is always some risk of fatigue and fracture, which may manifest itself in the life of a ball bearing. The most likely bearing failure, however, is lubricant failure causing the bearings to seize. Ball bearings overwhelmingly use lubricant oils and greases to ensure there isn't an excessive build-up of heat and friction between the races and the bearings. While a minimum amount of friction is necessary to ensure the bearings roll rather than slide (often specified as a minimum axial load), too much friction can cause the bearings to stick to the race and seize up, rather than allowing rolling.

Friction is inherently random and variable, as it is impacted by the different random surface asperities; as such it is incredibly difficult to model. The usual (but not exclusive) mechanism of lubricant failure is as followed: a high enough friction will heat the lubricant, which will reduce the

viscosity of the lubricant, which will increase the friction heating, and this feedback loop will continue until the friction between the bearing and the races is so great that the bearing seizes. If a bearing seizes during a critical application, the results can be catastrophic.

While it is impossible to truly know the exact nature of every bearing surface, empirical equations can be generated to determine the L_{10} life from a known bearing load, lubricant cleanliness, lubricant viscosity, and continuous bearing speed. The L_{10} life is defined as the number of revolutions a bearing can experience before a 10% chance of bearing failure. This effort is to study how tribological properties such as the lubricant film thickness [10–12] can serve to predict the change of failure after a single revolution, and thus estimate the L_{10} life.

2. Empirical Equations for L_{10} Life

In order to properly develop a numerical model for ball bearing failures, it is necessary to have empirical data on bearing failure to verify and validate it. In this aim, the L_{10} empirical equations provided by *Svenska Kullagerfabriken* (SKF) will be used as a baseline [13,14]; SKF is a Swedish company founded in 1907 and is currently the world's largest manufacturer of ball bearings. They have a bearing calculator that provides the L_{10} life in revolutions before the bearings have a 10% chance of failure. The core equation for L_{10} life is

$$L_{10} \quad = \quad A_{SKF} \cdot \left(\frac{C}{P}\right)^{\hat{p}} \cdot 10^6, \tag{1}$$

where C (N) is the *basic dynamic load rating*, P (N) is the *equivalent load*, and A_{SKF} is the *Life Modification Factor*. The value of $\hat{p}$ was found empirically, and it is *3* for spherical bearings and *10/3* for cylindrical bearings [15–17]. The value of A_{SKF} is a function of the the combined influence of load and contamination on fatigue β; and the viscosity ratio κ, which represents the lubrication conditions and their influence on fatigue. The basis for the $\left(\frac{C}{P}\right)^{10/3}$ component of equation 1 is based on empirical research of Lundberg and Palmgren [15–17].

The dimensionless value of κ is a ratio of the kinematic viscosity ν (m^2/s) over the rated viscosity ν_1 (m^2/s)

$$\kappa \quad = \quad \frac{\nu}{\nu_1}, \tag{2}$$

where ν_1 is a function of both the speed Ω_{rpm} and the average bearing diameter d_m (m)

$$\nu_1 \quad = \quad f(\Omega_{rpm}, d_m),$$
$$d_m \quad = \quad \frac{1}{2} \cdot (D + d),$$

where D (m) and d (m) represent the diameter of the inner and outer bearing race. The value of κ can range from 0.1 to 4.0, where $\kappa = 0.1$ represents total metal-on-metal contact, and $\kappa = 4.0$ represents a total lubricant coating. SKF did not publish their equation for ν_1, but it can be determined from the SKF bearing calculator. A least squared analysis was performed, and an estimated function for the rated viscosity ν_1 (m^2/s) is defined in equation 3

$$\nu_1 \quad = \quad 689.2653 \cdot 10^{-6} \cdot d_m^{-0.52706} \cdot \Omega_{rpm}^{-0.7565}, \tag{3}$$

where the mean diameter d_m is in meters and the bearing speed Ω_{rpm} is in revolutions per minute. Calculated values of ν_1 (m^2/s) are plotted in units of centistokes or mm^2/s in Figure 1.
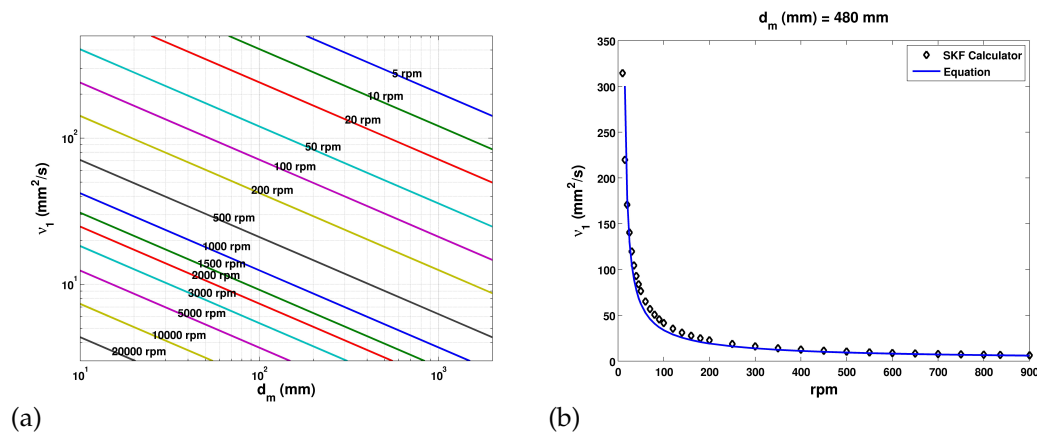
Figure 1. (a) Values of ν_1 (mm^2/s) calculated with equation 3 as a function of average bearing diameter d_m (mm) and Ω_{rpm}. (b) Comparison of equation 3 with the SKF calculator [13] values for d_m = 480 mm.

The other term necessary to determine A_{SKF} is the dimensionless coefficient β, which is the product of the cleanliness factor N_c and the safety factor ratio of the *fatigue load limit* P_u (N) over the equivalent bearing load P (N)

$$\beta = N_c \cdot \frac{P_u}{P}. \tag{4}$$

The cleanliness factor N_c ranges from 0.2 to 1.0, with 0.2 representing the dirtiest possible lubricant, and 1.0 representing a perfectly clean lubricant. In this analysis, the lubricant will be assumed to be clean, with $N_c = 1$. The equivalent load P (N) is a combination of radial and axial loads [18]

$$P = X_a \cdot F_a + X_r \cdot F_r, \tag{5}$$

where F_a (N) and F_r (N) are the axial and radial loads, and X_a and X_r are bearing specific coefficients. For example, for spherical thrust bearings X_a=1 and X_r=1.2.

The SKF website provides tables for the value of A_{SKF} as a function of β and κ, as well as a calculator tool, but no specific formula was given. For this reason, the least squared method was used, and a close match all throughout the permissible range of β and κ yielded the empirical equation 6

$$A_{SKF} = (C_{1,1} \cdot \kappa^3 + C_{2,1} \cdot \kappa^2 + C_{3,1} \cdot \kappa + C_{4,1}) \cdot (C_{1,2} \cdot \beta^3 + C_{2,2} \cdot \beta^2 + C_{3,2} \cdot \beta + C_{4,2}), \tag{6}$$

where the values of $C_{i,j}$ is tabulated in Table 1. Values of A_{SKF} calculated with equation 6 as a function of β and κ are plotted in Figure 2. Once the value of A_{SKF} is determined, it can be used in equation 1 to find the L$_{10}$ life, defined as the number of revolutions the bearing can undergo before encountering a 10% chance of failure. If one were to determine the probability of failure during a single revolution of the bearings P_f, it can easily be defined as

$$P_f = 1 - 0.9^{1/L_{10}}. \tag{7}$$

Table 1. Values of $C_{i,j}$ for equation 6.

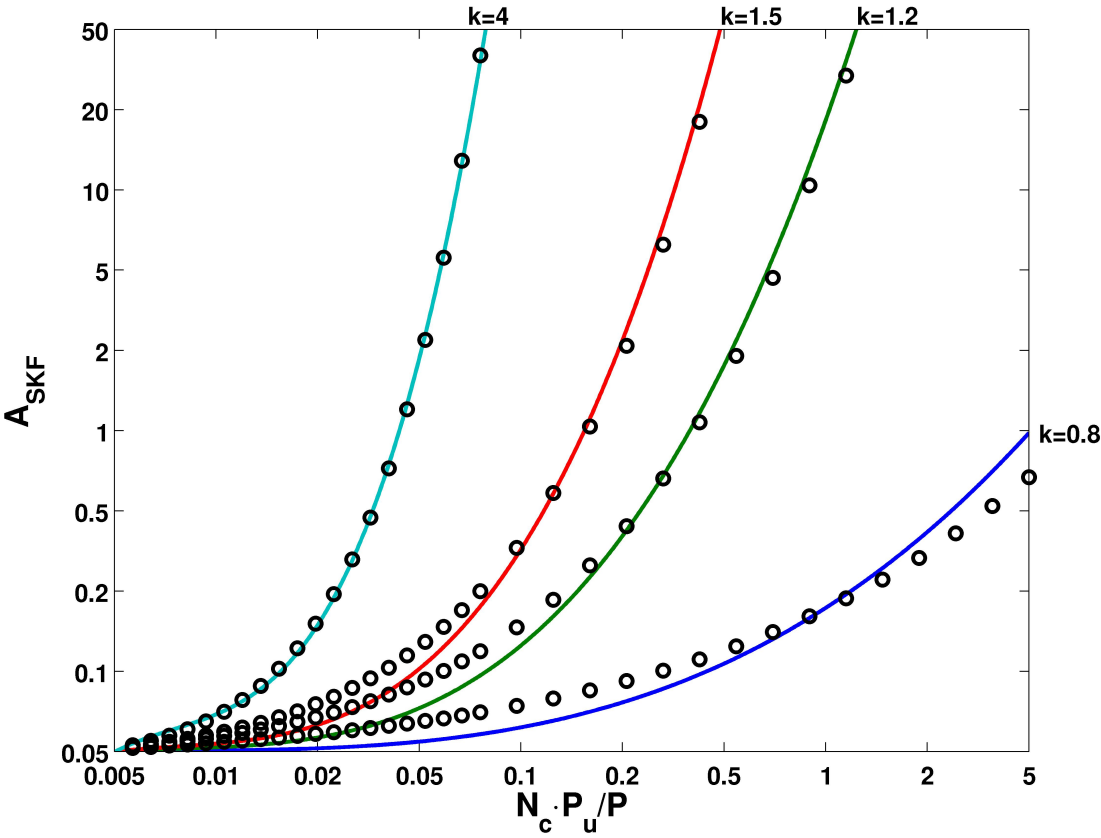|	i=1	i=2	i=3	i=4
j=1	-0.0559	0.3682	-0.3540	0.1012
j=2	8.43233	-8.2419	6.672284	-0.043546

Figure 2. Values of A_{SKF} calculated with equation 6 as a function of β and κ. Circles represent data points obtained with the SKF bearing calculator [13].

3. Tribological Predictions of L_{10} Life

Equation 1 can predict the L_{10}, but it gives no information as to the mechanics of the failure; it is a purely based on empirical data. In order to better understand the mechanism of failure, a model based on the tribological properties to find the values of L_{10} needs to be developed, with equation 1 being used to verify and validate this model.

Regardless of the L_{10} life, a ball bearing failure can happen; L_{10} life is really a function of the probability of failure in the face of random conditions such as surface asperities. The most common form of bearing failure is seizure, where excessive friction can yield increased heating, which reduces the lubricant viscosity, increasing the friction, until eventually the friction increases till it is high enough that the bearing seizes. Another potential cause of failure is a failure in fatigue; this will increase exponentially with increasing load relative to fatigue life. For the purpose of the analysis, the driving cause of failure will be treated as an excessively high increase in friction from the approximated average friction.

Friction is never constant in practice, it constantly fluctuates about a given average, therefore, this failure prediction model will be normalized to a given quantity of standard deviations away from the mean friction

$$
\begin{aligned}
P_f &= \frac{1}{2}\cdot erfc(\mu), \\
erfc(\mu) &= 1 - \frac{2}{\sqrt{\pi}}\cdot \int_0^{\mu} e^{-t^2/2}dt,
\end{aligned}
\tag{8}
$$

where *erfc* represents the complementary error function, and μ represents the Z-factor

$$
\mu = (x_i - x_m)/\sigma,
\tag{9}
$$

that corresponds to a given failure probability P_f for a single revolution. In equation 9, x_i (m) refers to a given asperities height over a given duration, x_i (m) refers to the mean asperities height of the roller bearing race, and σ (m) refers to the standard deviation of the asperities height for the given roller race. The relationship between μ and the L_{10} life is thus

$$
\mu = erfc^{-1}\{2\cdot(1 - 0.9^{1/L_{10}})\}.
\tag{10}
$$

While μ is a parameter for the probability of failure, it also is a representation of the mean coefficient of friction. According to Greenwood and Williamson's research [19–24], wear and friction (other than from fluid stresses) occur due to random asperities exceeding the thickness of the lubricant film [19–26]. Assuming the surface asperities height follows a normal distribution, the ratio of metal-on-metal contact A_{real}/A with the lubricant thickness should roughly follow

$$
\frac{A_{real}}{A} \approx exp(-\frac{h}{\sigma}),
\tag{11}
$$

where A_{real} (m^2) represents the true metal-on-metal contact area, A (m^2) represents the apparent (but not true) surface contact area, h (m) represents the lubricant film thickness, and σ (m) represents the RMS average asperities height. It is expected that the probability of lubricant failure will be a direct exponential function of the lubricant film thickness h (m) as described in equation 11.

4. First Parametric Study

A parametric study was conducted, utilizing the SKF NUP 2304-ECP cylindrical roller bearing. The radii of the individual cylindrical bearings are R=4.455 mm, and the length is 13.267 mm; the mean radius that the bearings rotate at is 72 mm. The fatigue load limit P_u is 4,800 N, and the basic dynamic load rating C is 47,500 N. The bearing is made of steel, so the Young's Modulus E_y will be 210 GPa,

120 and the poisson's ratio p will be 0.3. The parametric study would calculate both the L$_{10}$ life as defined
121 in equation 1, and compare it to the predicted lubricant film thickness [10–12,18,27–38], as well as the
122 relative fatigue load. The parametric study was conducted for a temperature ranging between 40°C
123 and 100°C, in increments of 2°C; an equivalent load ratio of 50 kN to 200 kN (in increments of 10
124 kN); and a bearing speed from 5,000 to 20,000 RPM, in increments of 1,000 RPM. With each of these
125 parameters, the L$_{10}$ life was calculated with equation 1 and equation 6, and an equivalent μ was found
126 with equation 10.
127   The next step was to predict the film thickness of the lubricant at the point of contact between the
128 bearings and the rollers during elastohydrodynamic contact [1,39–46]. In 1974, empirical equations by
129 Hamrock & Dowson [32] characterized the minimum h_0 (m) and central h_c (m) film thickness

$$h_{min} = 3.63R'(U_n^{0.68})(G_n^{0.49})(W_n^{-0.073})(1 - exp[-0.68\kappa_{ellipse}]), \tag{12}$$

$$h_c = 2.69R'(U_n^{0.67})(G_n^{0.53})(W_n^{-0.067})(1 - 0.61{\cdot}exp[-0.73\kappa_{ellipse}]), \tag{13}$$

$$U_n = \frac{\mu_0 U}{E'R'}, \tag{14}$$

$$G_n = \alpha_{PVC}E', \tag{15}$$

$$W_n = \frac{W}{E'R'^2}, \tag{16}$$

130 where h_{min} (m) is the minimum film thickness, h_c (m) is the central film thickness, U_n is the
131 dimensionless speed parameter, G_n is the dimensionless material parameter, W_n is the dimensionless
132 load parameter, $\kappa_{ellipse}$ is the ellipticity of the contact area, μ_0 (Pa-s) is the dynamic viscosity of the
133 lubricant at atmospheric pressure, α_{PVC} (Pa^{-1}) is the pressure viscosity coefficient, and U (m/s) is the
134 velocity of contact. The reduced Young's Modulus E' (Pa) and reduced radius R' (m) are for Hertz
135 contact equations for elastic deflection [1,47]. Assuming cylindrical rollers and a consistent material is
136 used, the equations for E' and R'

$$R' = \frac{R}{2}, \tag{17}$$

$$E' = \frac{E_y}{1 - p^2}. \tag{18}$$

137 where R (m) is the radius of the cylindrical bearing, and E_y (Pa) and p is the Young's Modulus and
138 Poisson's ratio of the bearing material.
139   If there is a given friction force that will cause the bearings to seize, and the friction is affected by
140 the ratio of the height of the surface asperities (which follow a normal distribution) over the lubricant
141 film thickness, an accurate equation for μ as a function of h_c (m) was realized with equation 19

$$\mu = X_1 + X_2{\cdot}exp(-\frac{h_c}{\sigma}) + X_3{\cdot}\sqrt{\frac{P}{P_u}}, \tag{19}$$

142 where σ was predicted as 1 μm RMS for the surface asperities, and P_u was defined as 4,800 N. Equation
143 19 incorporated two separate failure mechanisms, where X_2 is a coefficient for the lubricant seizure
144 based on friction (originating from Greenwood Williams theory [19–26]), and X_3 is a coefficient for the
145 rolling contact fatigue failure [15–17]. The fatigue life theory is an entirely different and independent
146 failure mechanism from lubricant seizure; equation 19 combines both potential failures into μ to obtain
147 an overall probability of bearing failure P_f during a given revolution.
148   The calculated value of μ found with equation 19 closely matches the value of μ found with
149 equation 10 (utilizing empirical equations 1 and 6), and is observed to match in Figure 3. The
150 coefficients for this particular design is $X_1 = 8.1130$, $X_2 = -3.1285$, and $X_3 = -1.0173$. By taking the
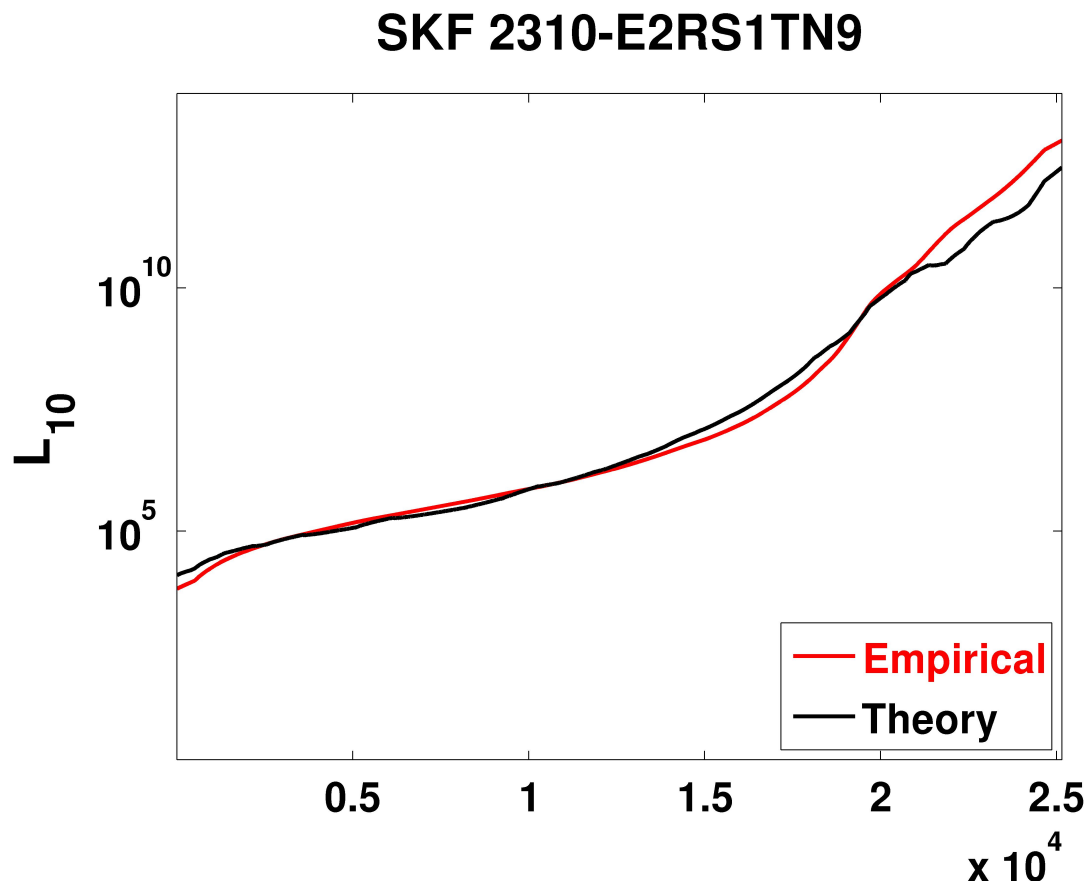
SKF 2310-E2RS1TN9

Figure 3. Calculated values of the L_{10} life, utilizing theoretical equation 19 and empirical equation 10, all for a parametric series of loads, speeds, and lubricant temperatures. The data is placed in ascending order of L_{10} life with the experimentally validated SKF empirical equations.

151 value of μ defined in equation 19, and using equations 7 and 8 one can predict the L_{10} life of a roller
152 bearing

$$L_{10} \;=\; \log{(0.9)}/\log{\{1 - 0.5{\cdot}erfc(\mu)\}}. \tag{20}$$

5. Second Parametric Study

154   A second parametric was conducted to see if varying the bearing size would affect the coefficients
155 for equation 19. The mean bearing radius was modeled from 30 mm to 500 mm. With a changing
156 bearing diameter, the radius of the rollers R (m) was consistently adjusted so 25 rollers in the bearings
157 would consistently fit within the roller bearing circumference

$$R \;=\; \frac{d_m{\cdot}\pi}{2{\cdot}N_r},$$

158 where $N_r = 25$ represents the number of cylindrical roller bearings. As observed in Figure 4, the first
159 two coefficients, X_1 and X_2 are a clear function of the inverse of the diameter

$$
\begin{aligned}
X_1 &= 5.1358 + \frac{0.2130}{d_m}, \\
X_2 &= 0.2071 - \frac{0.2330}{d_m}.
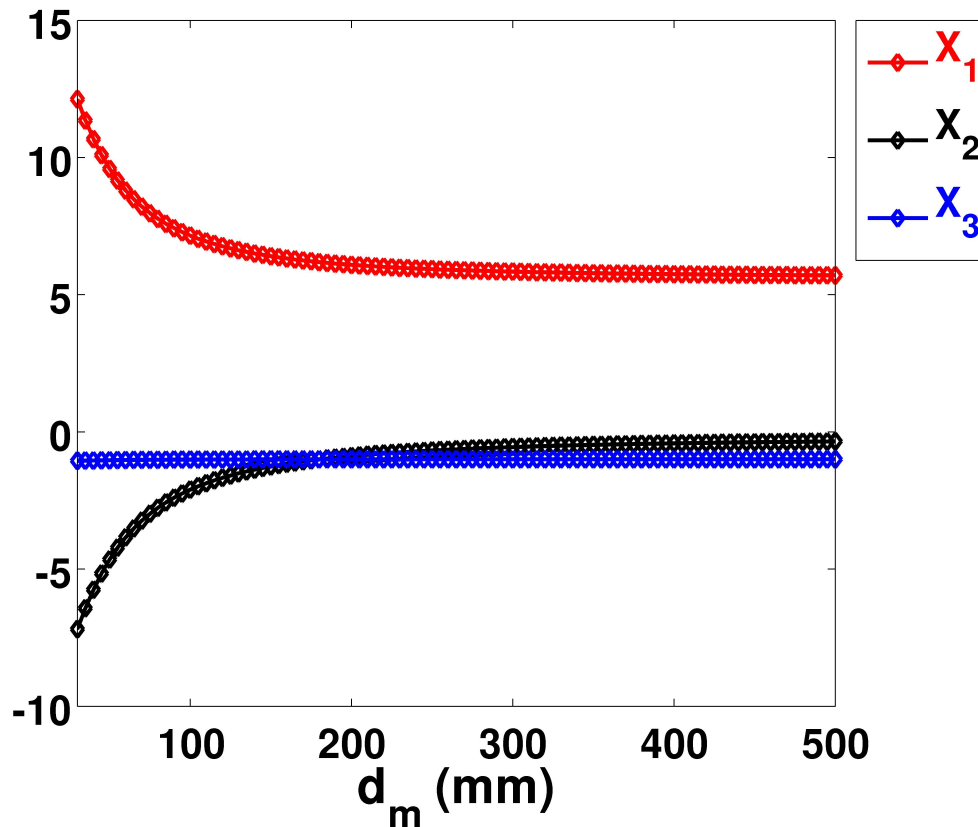\end{aligned}
\tag{21}
$$

Figure 4. Coefficients of equation 19 as a function of average bearing diameter d_m.

The third coefficient X_3 changes very little for changing average diameters d_m (m), it is predominantly an average of -1.00. By plugging the values of equation 21 into equation 19, one can get a comprehensive equation for the effective bearing life

$$\mu = 5.1358 + \frac{0.2130}{d_m} + (0.2071 - \frac{0.2330}{d_m}) \cdot exp(-\frac{h_c}{\sigma}) - \sqrt{\frac{P}{P_u}}, \tag{22}$$

$$L_{10} = \log(0.9)/\log\{1 - 0.5 \cdot erfc(\mu)\}.$$

The correlation coefficient R was predicted for all values of d_m (m) in equation 22, and consistently the correlation coefficient R, as plotted in Figure 5, exceeded 0.97.

6. Conclusion

In conclusion, a validated model to predict the probability of failures for roller bearings was developed. Empirical equations from *SKF* were developed from available data on commercial bearings to predict the L_{10} life based on known bearing conditions (lubricant viscosity, bearing speed, loads). These conditions were used, along with the roller bearing geometry, to predict the lubricant film thickness at the central point of contact. A thicker film thickness is expected to inherently have lower friction, and therefore a lower chance of lubricant failure, and a clear trend of lubricant thickness impacting the probability of bearing failure per revolution is observed. The relative load to the fatigue load is also taken into consideration; fatigue is considered a minor yet calculable influence on determining the bearing L_{10} life. This model demonstrates how the lubricant film thickness can be
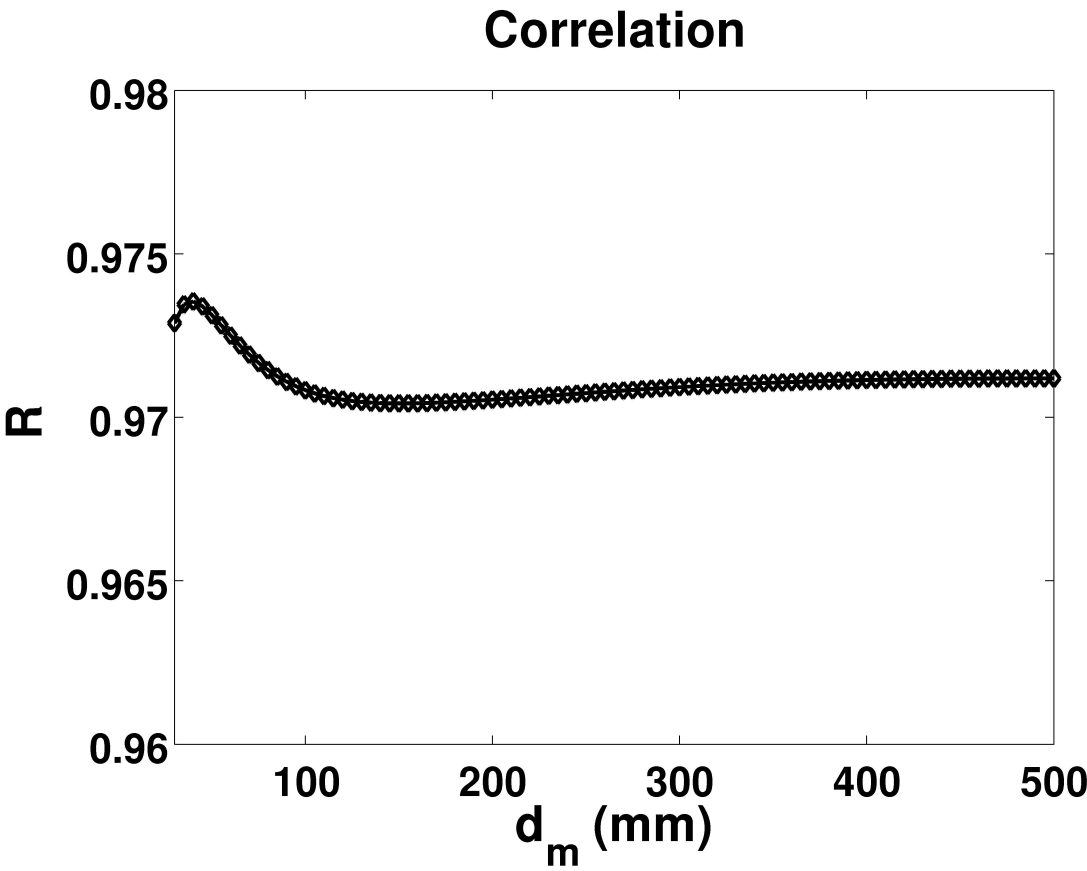
Figure 5. The correlation coefficient *R* of the SKF calculator data using equation 22, versus the SKF calculator results [13].

175   used to obtain a reasonable approximation for the life and probability of failure in seizing of a roller
176   bearing.

Abbreviations

183   The following abbreviations are used in this manuscript:

MDPI	Multidisciplinary Digital Publishing Institute
DOAJ	Directory of open access journals
BB	Ball Bearing
L_{10}	Number of revolutions before 10% chance of failure
COF	Coefficient of Friction

Bibliography

187   1.   Stachowiak, G.; Batchelor, A. *Engineering Tribology* 4th *Edition*; Butterworth-Heinemann: Oxford, UK, 2005.

188   2.   Gohar, R. *Elastohydrodynamics*; World Scientific Publishing Company: Singapore, 2002.

189   3.   Ranger, A.; Ettles, C.; Cameron, A. The Solution of the Point Contact Elasto-Hydrodynamic Problem.
190   *Proceedings of the Royal Society of London. Series A, Mathematical and Physical Sciences* **1975**, *346*, 227–244. doi:
191   10.1098/rspa.1975.0174.

192   4.   Blau, P. On the nature of running-in. *Tribology International* **2005**, *38*, 1007–1012. doi:
193   10.1016/j.triboint.2005.07.020.

194   5.   Hu, Y.; Li, N.; Tønder, K. A Dynamic System Model for Lubricated Sliding Wear and Running-in. *Journal*
195   *of Tribology* **1991**, *113*, 499–505. doi: 10.1115/1.2920651.

196   6.   Suzuki, M.; Ludema, K. The Wear Process During the "Running-ln" of Steel in Lubricated Sliding. *Journal*
197   *of Tribology* **1987**, *109*, 587–591. doi: 10.1115/1.3261511.

198   7.   Endo, K.; Kotani, S. Observations of Steel Surfaces Under Lubricated Wear. *Wear* **1973**, *26*, 239–251. doi:
199   10.1016/0043-1648(73)90138-5.

200   8.   Nanbu, T.; Yasuda, Y.; Ushijima, K.; Watanabe, J.; Zhu, D. Increase of Traction Coefficient due to Surface
201   Microtexture. *Tribology Letters* **2008**, *29*, 105–118. doi: 10.1007/s11249-007-9287-9.

202   9.   Wong, P.; Huang, P.; Wang, W.; Zhang, Z. Effect of geometry change of rough point contact due to
203   lubricated sliding wear on lubrication. *Tribology Letters* **1998**, *5*, 265–274. doi: 10.1023/A:1019162212773.

204   10.   Cann, P.; Spikes, H. In-contact IR spectroscopy of hydrocarbon lubricants. *Tribology Letters* **August 2005**,
205   *19*, 289–297. doi: 10.1007/s11249-005-7446-4.

206   11.   Jiang, P.; Li, X.M.; Guo, F.; Chen, J. Interferometry Measurement of Spin Effect on Sliding EHL. *Tribology*
207   *Letters* **2009**, *33*, 161–168. doi: 10.1007/s11249-008-9399-x.

208   12.   Reddyhoff, T.; Spikes, H.A.; Olver, A.V. Compression Heating and Cooling in Elastohydrodynamic
209   Contacts. *Tribology Letters* **2009**, *36*, 69–80. doi: 10.1007/s11249-009-9461-3.

210   13.   Svenska Kullager Fabriken AB. SKF Bearing Calculator **2017**.
211   http://webtools3.skf.com/BearingCalc/selectProduct.action.

212   14.   *SKF bearing maintenance handbook*; SKF Group, September 2011. ISBN 978-91-978966-4-1.

213   15.   Zaretsky, E.V. Rolling Bearing Life Prediction, Theory, and Application. *NASA Technical Report* **Nov 01, 2016**,
214   *NASA/TP-2013-215305/REV1, GRC-E-DAA-TN26137*. https://ntrs.nasa.gov/search.jsp?R=20160013905.

215   16.   Zaretsky, E.V. A Palmgren Revisited A Basis for Bearing Life Prediction. *NASA Technical Memorandum*
216   **May 1997**. https://ntrs.nasa.gov/archive/nasa/casi.ntrs.nasa.gov/19970025228.pdf.

217   17.   Rolling bearings: Dynamic load ratings and rating life. *International Organization for Standardization (DIN)*
218   **2007**. https://www.iso.org/standard/38102.html.

18. Nam, J.; Ryou, H.; Cho, S. A numerical model of rotating bearings for thermo-mechanical coupled analysis. *Proceedings of the 14th International Confernece on Simulation and Experiments in Heat Transfer and its Applications* **2016**, *106*, 25–31. doi: 10.2495/HT160031.

19. Greenwood, J.; Williamson, J. Contact of Nominally Flat Surfaces. *Proceedings of the Royal Society of London A* **1966**, *295*, 300–319. doi: 10.1098/rspa.1966.0242.

20. Bush, A.; Gibson, R.; Keogh, G. The Limit of Elastic Deformation in the Contact of Rough Surfaces. *Mechanics Research Communication* **1976**, *3*, 169–174. doi: 10.1016/0093-6413(76)90006-9.

21. Carbone, G. A slightly corrected Greenwood and Williamson model predicts asymptotic linearity between contact area and load. *Journal of the Mechanics and Physics of Solids* **2009**, *57*, 1093–1102. doi: 10.1016/j.jmps.2009.03.004.

22. McCool, J. Comparison of Models for the Contact of Rough Surfaces. *Wear* **1986**, *107*, 37–60. doi: 10.1016/0043-1648(86)90045-1.

23. Bush, A.; Gibson, R.; Thomas, T. The Elastic Contact of a Rough Surface. *Wear* **87-111**, *35*, 1975. doi: 10.1016/0043-1648(75)90145-3.

24. Persson, B. Contact mechanics for randomly rough surfaces. *Surface Science Reports* **2006**, *61*, 201–227. doi: 10.1016/j.surfrep.2006.04.001.

25. Finkin, E. Applicability of Greenwood-Williamson theory to film covered surfaces. *Wear* **1970**, *15*, 291–293. doi: 10.1016/0043-1648(70)90019-0.

26. Cann, P.; Ioannides, E.; Jacobson, B.; Lubrecht, A. The lambda ratio - A critical Re-examination. *Wear* **1994**, *175*, 177–188. doi: 10.1016/0043-1648(94)90181-3.

27. Crook, A. The Lubrication of Rollers. *Philosophical Transactions of the Royal Society of London, Series A, Mathematical and Physical Sciences* **1958**, *250*, 387–409. doi: 10.1098/rsta.1958.0001.

28. Archard, J. The Temperature of Rubbing Surfaces. *Wear* **1958**, *2*, 438–455. doi: 10.1016/0043-1648(59)90159-0.

29. Jaeger, J. Moving Sources of Heat and the Temperature at Sliding Contact. *Proceedings of the Royal Society N.S.W.* **1942**, *76*, 203–224.

30. Blok, H. Theoretical Study of Temperature rise at surfaces of actual contact under oiliness conditions. *Proceedings of the Institute of Mechanical Engineering, General Discussion on Lubrication* **1937**, *2*, 222–235.

31. Cameron, A.; Gohar, R. Theoretical and Experimental Studies of the Oil Film in Lubricated Point Contact. *Proceedings of the Royal Society of London. Series A, Mathematical and Physical Sciences* **1966**, *291*, 520–536. doi: 10.1098/rspa.1966.0112.

32. Hamrock, B.; Dowson, D. Isothermal Elastohydrodynamic Lubrication of Point Contacts, III Fully Flooded Results. *NASA Technical Note* **1976**, *D-8317*.

33. Hamrock, B.; Dowson, D. Isothermal Elastohydrodynamic Lubrication of Point Contacts, I Theoretical Formulation. *NASA Technical Note* **1975**, *D-8049*.

34. Hamrock, B.; Dowson, D. Isothermal Elastohydrodynamic Lubrication of Point Contacts, IV Starvation Results. *NASA Technical Note* **1976**, *D-8318*.

35. Dowson, D. Elastohydrodynamic and micro-elastohydrodynamic lubrication. *Wear* **1995**, *190*, 125–138. doi: 10.1016/0043-1648(95)06660-8.

36. Lugt, P.M.; Velichov, S.; Tripp, J.H. On the Chaotic Behavior of Grease Lubrication in Rolling Bearings. *Tribology Transactions* **2009**, *52*, 581–590. doi: 10.1080/10402000902825713.

37. van Zoelen, M.; Venner, C.; Lugt, P. Prediction of film thickness decay in starved elasto-hydrodynamically lubricated contacts using a thin layer flow model. *Journal of Engineering Tribology* **2009**, *223*, 541–552. doi: 10.1080/10402000902825713.

38. Venner, C.H.; Popovici, G.; Lugt, P.M.; Organisciak, M. Film Thickness Modulations in Starved Elastohydrodynamically Lubricated Contacts Induced by Time Varying Lubricant Supply. *ASME Journal of Tribology* **2008**, *130*, 041501. doi: 10.1115/1.2958069.

39. Venner, C.; van Zoelen, M.; Lugt, P. Thin layer flow and film decay modeling for grease lubricated rolling bearings. *Tribology International* **2012**, *47*, 175–187. doi: 10.1016/j.triboint.2011.10.019.

40. Fillot, N.; Berro, H.; Vergne, P. From Continuous to Molecular Scale in Modelling Elastohydrodynamic Lubrication: Nanoscale Surface Slip Effects on Film Thickness and Friction. *Tribology Letters* **September 2011**, *43*, 257–266. doi: 10.1007/s11249-011-9804-8.

41. Guo, F.; Wong, P.L.; Geng, M.; Kaneta, M. Occurrence of Wall Slip in Elastohydrodynamic Lubrication Contacts. *Tribology Letters* **May 2009**, *34*, 103–111. doi: 10.1007/s11249-009-9414-x.

42. Krupka, I.; Bair, S.; Kumar, P.; Svoboda, P.; Hartl, M. Mechanical Degradation of the Liquid in an Operating EHL Contact. *Tribology Letters* **2011**, *41*, 191–197. doi: 10.1007/s11249-010-9698-x.

43. Marko, M. The Tribological Effects of Lubricating Oil Containing Nanometer-Scale Diamond Particles. *Columbia University* **2015**, *PhD Thesis*. doi: 10.7916/D8FF3R6G.

44. Marko, M.; Kyle, J.P.; Wang, Y.S.; Terrell, E.J. Tribological investigations of the load, temperature, and time dependence of wear in sliding contact. *PLOS One* **2017**, *12*. doi: 10.1371/journal.pone.0175198.

45. Marko, M.D.; Kyle, J.P.; Branson, B.; Terrell, E.J. Tribological Improvements of Dispersed Nano-Diamond Additives in Lubricating Mineral Oil. *Journal of Tribology* **2015**, *137*, 011802. doi: 10.1115/1.4028554.

46. Marko, M.D.; Kyle, J.P.; Wang, Y.S.; Branson, B.; Terrell, E.J. Numerical and Experimental Tribological Investigations of Diamond Nanoparticles. *Journal of Tribology* **2016**, *138(3)*, 032001. doi: 10.1115/1.4031912.

47. Johnson, K. *Contact Mechanics*; Cambridge University Press: 40 W 20th St, New York NY 10011, 1987.